



# **Contamination Knowledge Report:**

## **Coordinated study of contaminated KBr window**

**Report prepared by: Scott Messenger**  
**Analysts: Lindsay Keller (FTIR)**  
**Yulia Goreva (ToF-SIMS)**  
**Michael Callahan (DART)**  
**Jason Dworkin (GCMS)**  
**Simon Clemett ( $\mu\text{L}^2\text{MS}$ , SEM)**  
**Jamie Elsila (Organics)**  
**Jason Dworkin, MPS**  
**Harold C. Connolly Jr. MSS**

### **Summary**

During the course of a spectral study of Murchison fine grained matrix, an outgassing event took place that left a film of material on the surface of a KBr window in the apparatus. This material was examined by several different techniques to determine its nature and origin. The results of this study indicate that the residue mainly consists of potassium nitrate ( $\text{KNO}_3$ ), with minor amounts of high molecular weight insoluble N-bearing organic molecules and  $(\text{AlO}_x)_\text{N}$ .  $\text{KNO}_3$  is not a constituent of primitive meteorites but it is used in industrial materials including fertilizer, explosives, preservatives, and propellants. The most likely origin of this material is a contaminant introduced into the sample. This report summarizes and includes material from reports provided by the analysts.

### **Background**

FTIR spectra were obtained from several meteorite samples heated to  $\sim 150^\circ\text{C}$  under high vacuum conditions to simulate the surface of an airless body at University of Oxford Planetary Spectroscopy Facility. While analyzing a  $<150\ \mu\text{m}$  grain size separate of Murchison matrix, a strong outgassing event occurred. This followed uneventful measurements of coarse grained Murchison and various size fractions of Allende and NWA502 meteorites performed over the preceding two week period. The outgassing problem was so strong that the instrument needed to be extensively cleaned before it could achieve acceptable vacuum levels.

The KBr window examined here was stored in atmosphere for several weeks prior to being shipped to JSC, where it has since been stored in a  $\text{N}_2$ -purged sample cabinet.

### **Analyses performed**

Visual inspection of the KBr window revealed a semi-transparent grey film over the entire surface. The window was cleaved by hand with a stainless steel razor blade into  $\sim 1\ \text{cm}^2$  sections for analysis by the following techniques: optical microscopy, scanning electron microscopy (SEM), Fourier transform infrared spectroscopy (FTIR), gas chromatography mass

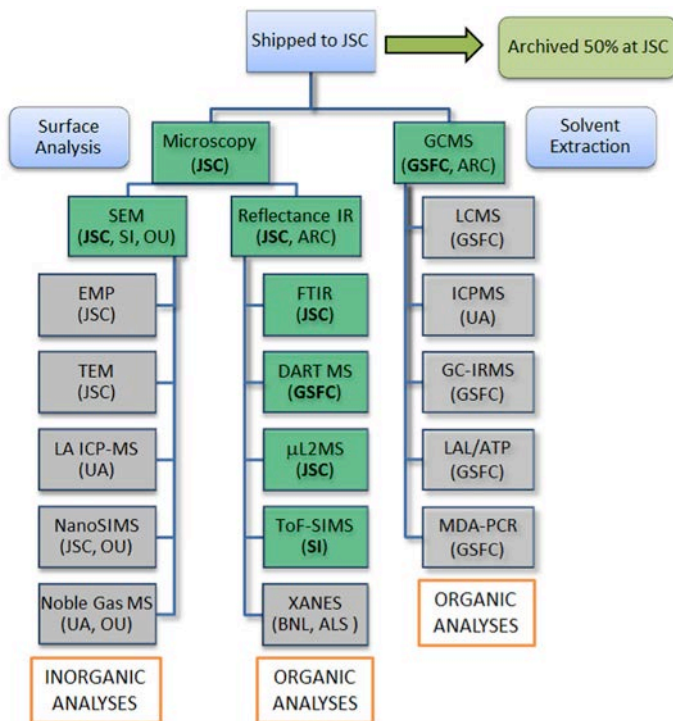


Fig. 1: Techniques used to examine the composition of material deposited onto the KBr window (green boxes). Other techniques available to members of the OSIRIS-REx sample analysis team are also listed (grey boxes).

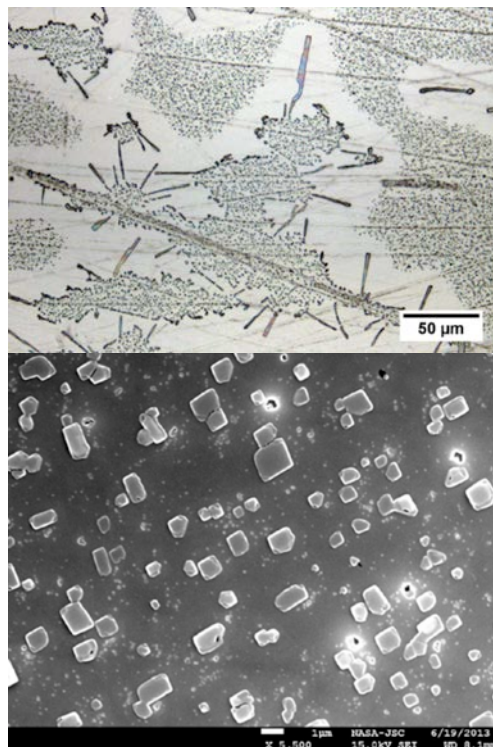


Fig. 2 (top): Optical microscope image of the surface of the coated KBr window. (bottom): SEM image of the surface of the coated KBr window.

spectrometry (GCMS), direct analysis real time (DART) mass spectrometry, time of flight secondary ion mass spectrometry (ToF-SIMS), and microprobe two-step laser ionization mass spectrometry  $\mu\text{L}^2\text{MS}$  (Fig. 1). With the exception of a few pieces that were first inspected by optical microscopy, all other analyses were performed on separate samples of the KBr window. The GCMS, ToF-SIMS, FTIR, DART, and  $\mu\text{L}^2\text{MS}$  measurements were performed both on samples of the coated window and a clean blank KBr window as a control.

## Results: Optical and SEM imaging

Optical microscope imaging revealed that the interior (vacuum) side of the KBr window had a translucent coating consisting of numerous closely packed crystallites with sizes on the order of 1  $\mu\text{m}$  (Fig. 2). Frequently extending from outer periphery of these islands are long thin rectangular crystals, 10's to 100's of microns long and typically 1-5  $\mu\text{m}$  wide. The crystals were observed to lie on, and extend above, the *KBr* substrate with no visual evidence of dissolution or etching of the underlying *KBr*. This implies the coating to be a depositional and not an erosional feature. The crystallites showed a euhedral cubic habit and were epitaxially aligned along the underlying *KBr* [100] crystallographic axis. During the course of SEM analysis the crystals readily decomposed induced by electron beam heating as evidenced by significant deflation of the crystal volume.

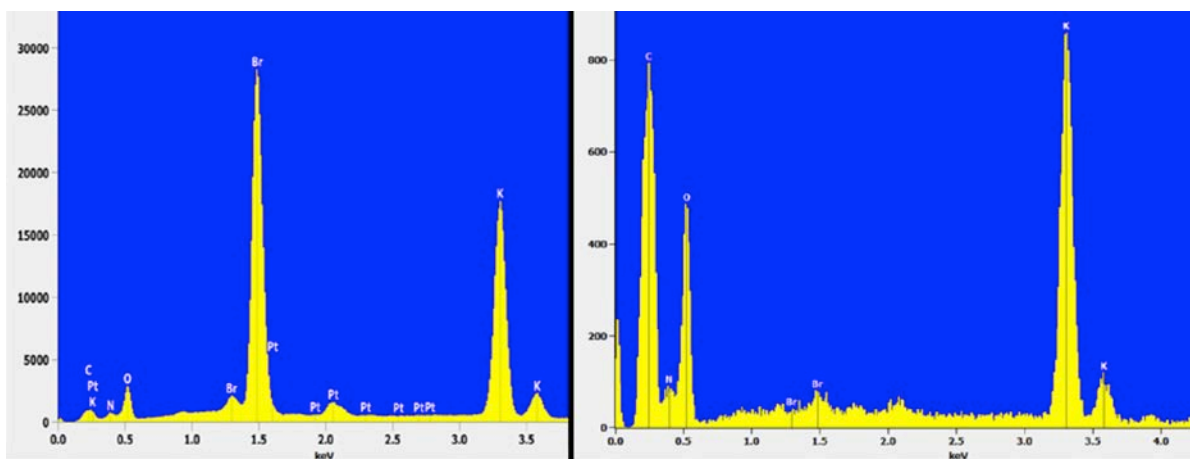


Fig. 3: SEM EDX spectra obtained from crystals removed from the KBr surface (left) and KBr window-free crystallites (right).

### Results: Elemental composition

Major and minor element abundances were determined by SEM-EDX analysis of Pt or C coated samples. Initially analyses were conducted directly on the KBr substrate and showed spectra dominated by K and Br with small peaks from O, N and minor C. The prominent K and Br were attributed to the KBr substrate. Later analysis were performed on crystallites that had been removed from KBr substrate and mounted on Au foil. These analyses showed that the crystallites are composed primarily of K, O and N with trace to minor amounts of Al, P and Si. Crystal bond adhesive was used to extract crystals from the KBr substrate so it was not possible to assess the C abundance.

### Results: FTIR spectroscopy

Both the reflectance and transmission IR spectra are dominated by bands that correspond to nitrate groups (the strong doublet at  $\sim 1370\text{ cm}^{-1}$  and the satellites at  $\sim 830, 1640$  and  $1790\text{ cm}^{-1}$ ). It is not possible to determine the cation that is bonded to the nitrate anion in the coating from these spectra alone. In addition to the nitrate bands, weaker bands from aliphatic hydrocarbons occur at  $2850$  and  $2920\text{ cm}^{-1}$ . There is also a weak, but broad O-H band that occurs in the  $3200\text{-}3600\text{ cm}^{-1}$  region.

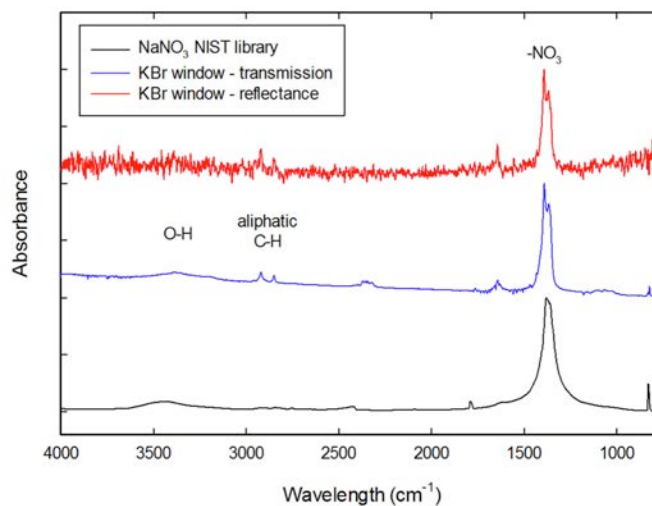


Fig. 4: FTIR spectrum of KBr window compared with NIST reference standard  $\text{NaNO}_3$ .

## Results: Chemical analysis by GCMS, ToF-SIMS, DART, & $\mu$ L2MS

Detailed chemical analyses of the residue were obtained by solvent extraction (GCMS) and surface analysis techniques (ToF-SIMS, DART, &  $\mu$ L2MS). These techniques are complementary to each other and provide different types of constraints on the nature of the residue. Briefly: GC-MS can be used to identify specific soluble or derivatizable organic compounds in macroscopic samples; ToF-SIMS provides broad chemical trends on  $\mu$ m-spatial scales with little molecular specificity; DART can be used to identify specific surface-deposited molecules on 1000  $\mu$ m spatial scales,  $\mu$ L2MS can be used to identify specific organic molecules on 10  $\mu$ m spatial scales.

## Results: GCMS

Samples of the clean and coated KBr windows were separately derivatized and the extracted organic compounds were analyzed by GC-MS. A comparison of the chromatograms from the coated and blank KBr windows did not reveal any peaks that were unique to either. However, there was a higher abundance of a short derivatized polyethylene glycol-like compound (probably diethylene glycol) in the control than the coated window. These results suggests that whatever the residue is on the KBr window, it is not soluble in MTBSTFA:DMF, or does not contain any soluble MTBSTFA:DMF-derivatizable compounds.

## Results: ToF-SIMS

ToF-SIMS spectra were obtained from 500x500  $\mu$ m areas in positive and negative polarity. Trace inorganics and organic species including plasticizers and polycyclic aromatic hydrocarbons (PAHs) were observed on both the coated and blank KBr windows. Species only observed on the coating include Na<sup>+</sup>, P<sup>+</sup>, F<sup>-</sup>, and SO<sup>3-</sup>. In addition, bonding of K to C (CO) compounds were also observed (K<sub>3</sub>C<sub>2</sub>O<sub>2-4</sub>). The coated window also presented complex C-H-O, S, N-bearing compounds that reach high molecular weight (Fig. 5).

Definitive peak assignments in ToF-SIMS spectra to specific species is usually not possible due to low mass resolving power and high degrees of fragmentation due to interaction with the primary ion beam.

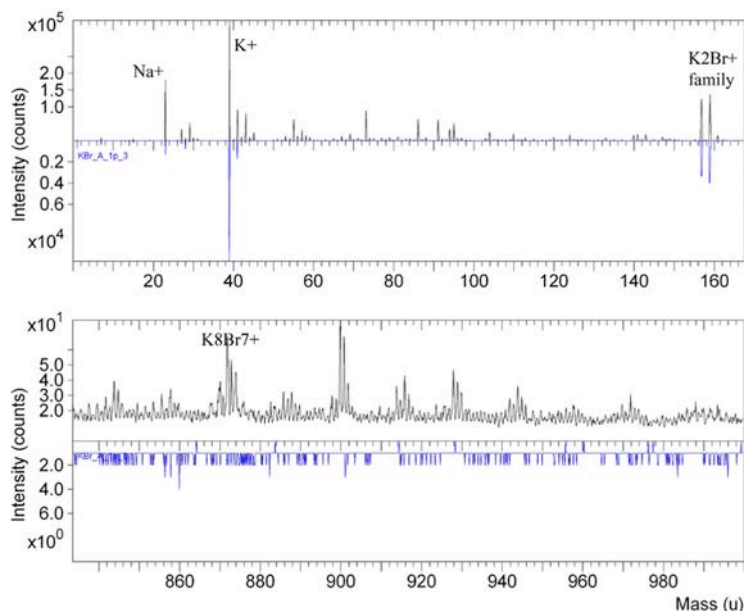


Fig. 5: Summed ToF-SIMS spectra showing low molecular weight region (top) and high molecular weight region (bottom). Spectrum of blank is shown inverted (blue).

However, analysis of fragmentation patterns, exact masses, isotopomer distributions and reference to spectral libraries may enable peak assignments. In this sample, the following species were identified: polyethylene glycol, certain amino acids, C<sub>2</sub>SN, SNOH, C<sub>4</sub>H<sub>2</sub>N, and C<sub>2</sub>H<sub>8</sub>N<sub>3</sub>O. Some of these species, such as C<sub>2</sub>SN and C<sub>4</sub>H<sub>2</sub>N are not stable compounds and are probable fragmentation products formed by sputtering and ionization processes during the analysis.

## Results: $\mu$ L2MS

Mass spectra of the KBr window surface were acquired by  $\mu$ L2MS from 10  $\mu$ m spots. Resultant spectra represent the summed signal from multiple individual point analysis covering an area of  $\sim$ 1000  $\mu$ m<sup>2</sup>. Two separate sets of spectra were acquired by using UV (266 nm) and VUV (118 nm) photoionization (Fig. 6). The spectra obtained by 266 nm laser ionization are highly sensitive and selective for PAH molecules, while spectra obtained by 118 nm laser ionization provide a much more general window for nearly any class of organic species. In both cases some information on inorganic species and elements with particularly low ionizations are also obtained.

The dominant mass peaks in the 266 nm spectrum are all below 100 amu and correspond to simple inorganic ions Al<sup>+</sup>, K<sup>+</sup> and Al<sub>2</sub>O<sup>+</sup>. Above 100 amu a number of weak molecular ion peaks are present and are consistent with 1- and 2-ring aromatics such as styrene (C<sub>6</sub>H<sub>5</sub>CH=CH<sub>2</sub>; 104 amu) and naphthalene (C<sub>10</sub>H<sub>8</sub>; 128 amu).

Spectra obtained by 118 nm ionization are dominated by a molecular peak at  $\sim$ 126.9 amu. The mass deficit of this species rules out an organic (H-bearing) molecule. The exact mass of this peak was determined to be (M = 126.9159  $\pm$  0.0013 amu) and this peak is accompanied by

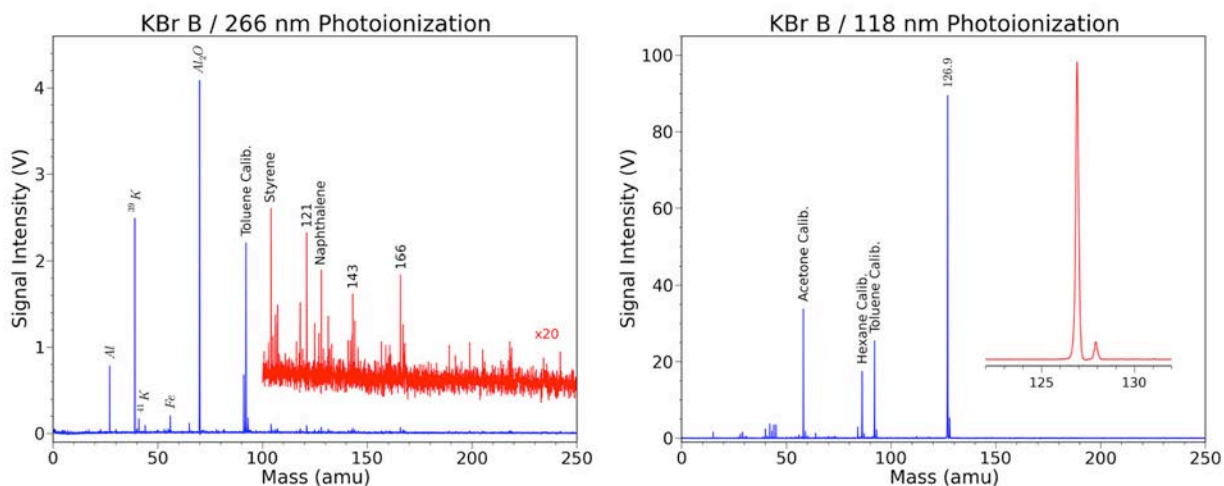


Fig. 6: Summed ToF-SIMS spectra showing low molecular weight region (top) and high molecular weight region (bottom). Spectrum of blank is shown inverted (blue).

an isotopomer peak at  $M + 1.0120 \pm 0.0018$  amu. The exact mass and isotopomers peak is consistent with the doubly charged cluster ion K(AlO)<sub>5</sub>. Alternative peak assignments including iodine and C-bearing species are definitively ruled out by the isotopomer distribution and exact masses of these two peaks.

## Results: DART

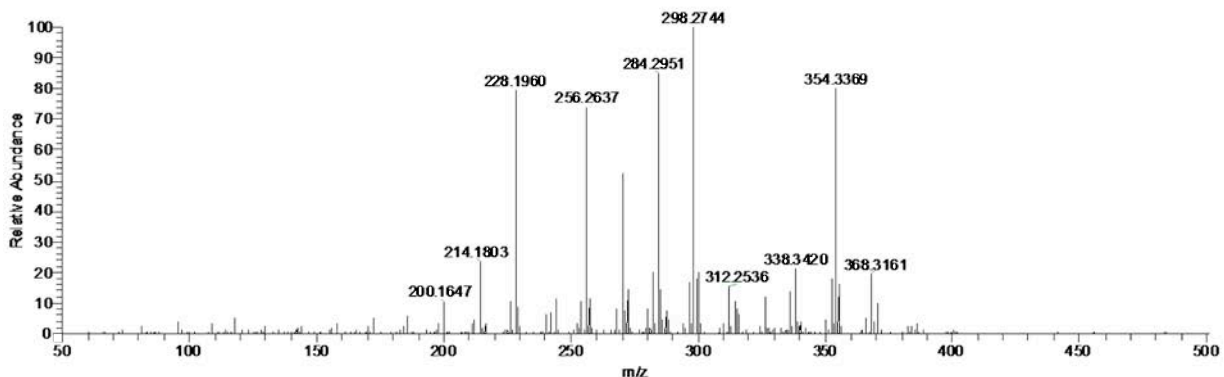


Fig. 7: DART spectra showing a distribution of intermediate weight organic molecules on the surface of the coated KBr window.

A distinct distribution of mass peaks was observed on the coated KBr window that did not occur on the blank. These molecules spanned primarily from  $m/z$  200 to  $m/z$  400, which is consistent with molecular-weight compounds that would likely remain on the KBr surface upon initial sublimation of Murchison meteorite. An elemental composition was assigned for the 10 most intense mass peaks and is shown in Table 1. These organic compounds all contain carbon, hydrogen, oxygen, and nitrogen and their molecular formulae suggest fairly complex organic species, which is consistent with numerous past studies of Murchison meteorite (including M u r c h i s o n s u b l i m a t e s ) .

m/z	Relative Intensity	Theo. Mass	Delta (ppm)	Composition, $[M+H]^+$
298.2743	100	298.2741	0.93	$C_{18}H_{36}O_2N$
284.2951	84.29	284.2948	0.99	$C_{18}H_{38}ON$
228.1960	80.64	228.1958	0.67	$C_{13}H_{26}O_2N$
354.3368	78.39	354.3367	0.51	$C_{22}H_{44}O_2N$
256.2637	74.64	256.2635	0.76	$C_{16}H_{34}ON$
270.2430	51.77	270.2428	1.07	$C_{16}H_{32}O_2N$
214.1803	23.56	214.1802	0.8	$C_{12}H_{24}O_2N$
338.3420	21.12	338.3417	0.64	$C_{22}H_{44}ON$
282.2794	19.74	282.2791	1.01	$C_{18}H_{36}ON$
300.2900	19.68	300.2897	0.86	$C_{18}H_{38}O_2N$

Table 1: DART accurate mass measurements for the 10 most intense mass peaks in Fig. 7.

## Discussion

Considering these analyses together, we can conclude that most of the mass deposited consisted of  $KNO_3$ . This is based upon the optical and SEM imaging studies that showed that the deposit was a cubic crystalline material that was epitaxially oriented on the sample surface (thus mostly one substance). FTIR spectra show a strong IR feature consistent with a nitrate anion. EDX elemental analysis of the crystals indicates that the cation bound to the nitrate is K.  $KNO_3$  is not a constituent of primitive meteorites but it is used in a variety of industrial materials. Therefore, it is likely that this material is a contaminant. Other compounds that are likely to have been associated with the condensate include  $K(AlO)_5$  identified by  $\mu L2MS$  and  $K_3C_2O_{2-4}$  identified by ToF-SIMS. These accessory compounds give further clues to the origin of the contaminant. In particular, the presence of aluminum oxide bound to potassium is suggestive

of a relationship with pyrotechnics or flash powder. In some preparations of these types of explosives  $\text{KNO}_3$  acts as an oxidizer and aluminum and sulfur are reducing agents. This combination of materials is considered a low grade explosive that is often made by amateurs. Other potential  $\text{KNO}_3$ -bearing contaminants include fertilizer, preservatives, and propellants.

Although there are many conceivable sources of  $\text{KNO}_3$  as a contaminant, it is not obvious how it could be evolved and condensed on the KBr window. This material does not sublime under vacuum, is not volatile and its melting point (334 °C at STP) is well above the maximum temperature experienced by the meteorite sample (~150 °C). One possible scenario is that the  $\text{KNO}_3$  was bound together with other nitrate salts that together had a lower melting point. Experiments have shown that  $\text{KNO}_3$  may evaporate with low levels of decomposition. Alternatively, the  $\text{KNO}_3$  could have formed in the vapor phase and condensed on the KBr substrate. But it is even more difficult to construct a reasonable scenario for this to occur from the types of volatile compounds known to exist in primitive meteorites.

All of the mass spectrometric methods employed also showed the presence of trace organic and inorganic species that probably derived from the Murchison meteorite (intermediate weight organics), possibly from terrestrial contamination of the meteorite or KBr window (amino acids), and even packaging of the sample and KBr window (plasticizers and Teflon).

## **Implications for Contamination Knowledge and Sample Analysis**

This investigation was a useful practical exercise in preparation for the contamination knowledge effort that will soon be underway during ATLO and for the future coordinated analyses of returned samples from asteroid Bennu.

*Contamination knowledge* will perform the minimum analyses necessary to determine whether contaminants significantly impact priority science studies. If necessary, specialized instruments will be called upon to delve to a deeper level of detail for the material properties. Initial examinations of witness materials will be performed by optical microscopy, infrared spectrometry, and scanning electron microscopy.

Each of the general survey instruments (microscopy, SEM, FTIR) provided critical constraints that led to the identification of  $\text{KNO}_3$  as the main contaminant. Yet, this initial identification left open the question of where the  $\text{KNO}_3$  may have come from. To answer this question, we turned to specialized chemical analysis instruments. GCMS, DART, and  $\mu\text{L}^2\text{MS}$  ruled out a significant organic component and  $\mu\text{L}^2\text{MS}$  yielded a potentially critical clue from identifying the pervasive K(AIO) peak.

It is useful to directly compare the types of information provided by the specialized chemical analytical instruments when analyzing the same material. Each of these techniques possesses strengths and shortcomings that can help to guide under what circumstances they should be used for contamination knowledge.

**GCMS:** This is a well-established technique that reliably identifies specific soluble organic species. The major shortcoming of this technique is that the requisite sample size is relatively large and cannot be used for particle studies. In this study the GCMS measurements were useful in confirming that soluble organics were not a major component of the residue.

**DART:** This is a relatively new technique that has two major advantages: ease of use (thus low cost) and ability to identify specific molecular formulae of even high mass organic compounds. Shortcomings include the low spatial resolution (millimeter-scale). In this study,

intermediate mass organic compounds were identified that may have evolved from the Murchison sample, but this analysis did not appear to provide constraints on the residue.

**ToF-SIMS:** This technique is most useful for analyzing trace materials on the uppermost surface of a sample. A significant shortcoming is that most molecules are fragmented and spectra of complex materials are often difficult to interpret. In this study, the ToF-SIMS spectra included peaks that were probably associated with the main contaminant.

**$\mu$ L2MS:** This technique is uniquely capable of definitively identifying low to intermediate-weight molecular compounds on microscopic scales without significant fragmentation. A shortcoming (compared with DART and GCMS) is that high molecular weight compounds are measured at low mass resolving power, leaving the specific molecular formula uncertain.

Among these techniques, GC-MS is considered the most useful for organic analysis of large samples, due to the ability to definitively identify soluble organics. DART may have great utility for identifying large molecular weight organic compounds deposited over large surface areas ( $\sim 1 \text{ mm}^2$ ).  $\mu\text{L}^2\text{MS}$  is the most useful technique for molecular analysis of small particles or regions 10-100  $\mu\text{m}$  in scale. ToF-SIMS can be useful for measuring trace organic and inorganic contaminants in thin surface coatings ( $\ll 1 \mu\text{m}$ ), but offers a lower degree of molecular specificity of the other chemical analysis tools. It is important to stress that each of these techniques offers chemical information at very different mass and spatial scales. The optimal approach to use will be guided by constraints derived from lower level optical and spectroscopic investigations.



# Contamination Knowledge Report

Jamie Elsila  
Jason Dworkin  
6 December 2013

## Summary

The KBr window samples do not contain unique detectable amounts of MTBSTFA-DMF-soluble or derivatizable compounds.

## Introduction

Samples of KBr windows from the thermal vacuum analysis of the Murchison meteorite were provided in baked centrifuge tubes. Two samples (KBr A and KBr B) were provided; one was a blank and the other contained residue from the Murchison test.

The two samples were derivatized directly with 4:1 N-tert-Butyldimethylsilyl-N-methyltrifluoroacetamide:dimethyl formamide (MTBSTFA:DMF), a silylation reagent commonly used for silylation to create volatile derivatives of organic compounds from species which contain one or more labile H (Fig 1). We added 50  $\mu\text{L}$  of MTBSTFA:DMF to each centrifuge tube, making sure to rinse both sides of the KBr window fragments with the reagent. Tubes were capped and heated in a heating block at 75  $^{\circ}\text{C}$  for 45 minutes, then cooled to room temperature. Gas chromatograph-mass spectrometer (GC-MS) analyses were performed on 1  $\mu\text{L}$  injections of the derivatized sample (see Appendix A).

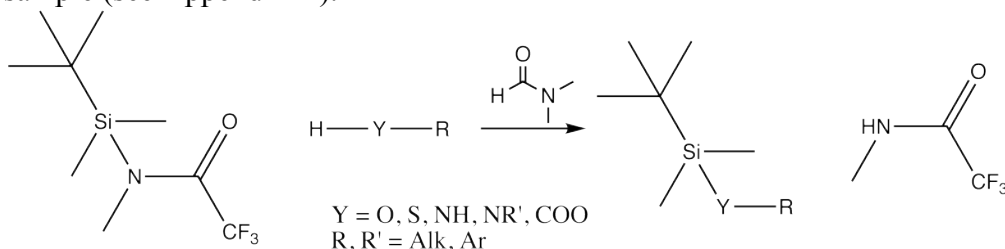


Fig 1. MTBSTFA reaction

## Results

A comparison of the chromatograms from KBr A, KBr B, and MTBSTFA:DMF did not reveal any peaks that were unique to either KBr A or KBr B. There was a higher abundance of a short derivatized polyethylene glycol-like compound (probably diethylene glycol) in KBr B, than present in KBr A (Fig 2). Diethylene glycol is a common in industrial and consumer products, and could have been introduced irrespective of the Murchison sample. This suggests that whatever the residue is on the KBr window, it is not soluble in MTBSTFA:DMF, or does not contain any soluble MTBSTFA:DMF-derivatizable compounds.

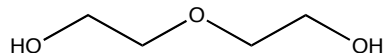


Fig 2. Diethylene glycol

### **Potential future tests:**

If desired, additional fragments of the KBr windows could be tested via the following methods:

- 1) Direct Analysis in Real Time (DART) coupled with an Orbitrap mass spectrometer. This would allow sampling directly from the solid sample, allowing the analysis of insoluble compounds. Unfortunately, the instrument is currently awaiting repairs.
- 2) Water or methanol extraction of the samples would dissolve much of the KBr window and allow for analysis of water-soluble compounds. A water extract could then be analyzed via liquid chromatography with electrospray ionization and time-of-flight mass spectrometry. This can provide a formula, but not necessarily a structure. The presence of soluble KBr would complicate the analysis.
- 3) Pyrolysis-GC-MS. Fragments of the KBr windows could be crushed and then pyrolyzed, with the resulting gases separated via GC-MS. This would allow analysis of insoluble compounds, but would indicate what the compounds degrade to upon pyrolysis, not necessarily their initial form.

### **Appendix A**

Instrumentation: The GC-MS system was a Thermo Scientific Trace 1310 gas chromatograph coupled with a Thermo TSQ8000 triple quadrupole mass spectrometer operated in single quadrupole mode, outfitted with a TG-5SilMS column. The initial temperature was 50 °C, held for two minutes, then ramped at 10 °C/minute to 300°C.